LUND UNIVERSITY
Faculty of Science

Numerical simulations of contact geometry effects on transport properties of semiconductor nanowires

Emil Johansson

Thesis submitted for the degree of Bachelor of Science
Project duration: 2 months

Supervised by P. Samuelsson

Department of Physics
Division of mathematical physics
May 2016

Abstract

This Bachelor thesis presents numerical simulations of lead-geometry effects in low temperature nanowires. The method combines an effective mass approximation with the numerical finite difference method scheme to produce transmission coefficients. The quantum transport package Kwant [1] facilitates the construction and calculations of transmission coefficients through scattering regions connected with semi-infinite leads. The transmission coefficients are then linked to the conductance via the Landauer-Büttiker formalism.

3D simulations suggest that contact geometry effects can cause a drop in conductance before the onset of a new transport mode. 2D simulations show that increasing the length of nanowire in contact with the leads increases the conductance through the nanowire. Further, the finite length of the nanowire causes resonances to form at energies related to the eigenenergies of the Hamiltonian describing the unperturbed wire without leads. An increased length of the nanowire combined with wide contact results in the reappearance of the conductance steps associated with the corresponding infinite wire.

However, different effective masses in the metal and semiconductor materials cause errors, due to transversal states in the leads get erroneous energies. Further, to make quantitative fitting to experimental conductance measurements, this issue needed to be addressed.

Acknowledgements

I want to thank my supervisor Peter Samuelsson for his support, encouragement, and positive attitude. All the way from his first positive response to my email asking for the opportunity do a summer project with Peter as my supervisor in the summer of 2015, until now a year and a bachelor project on the same subject later. Further, Peter has in the form of my supervisor been a vital part in this thesis with his knowledge and experience.

I also want to acknowledge the importance of the work done by Oscar Erlandsson in his bachelor thesis presented January 2016 [2] and the importance of our discussions about more technical Kwant specific challenges. I also want to thank the people at Mathematical Physics. From them I have learned much about science and life.

Finally, I want to thank Desiré Nilsson for the support and understanding during these past years of physics studies. During which I have learned that we are nothing without those we love.

Abbreviations

NWs Nanowires

nm Nanometer, 1nm = 10^{-9}m

EMA Effective mass approximation

FDM Finite difference method

TB Tight binding

PDEM Position dependent effective mass

Contents

1 Introduction

On the boundary between classical physics and quantum mechanics is mesoscopic physics. Mesoscopic physics deals with modeling systems that are too small for classical physics and to large to solve the exact Schrödinger equation. This field of research became particularly interesting when, during the 1980s, it became possible to create systems experimentally in the nanometer (nm) size range. Mesoscopic physics attracted further interest as electrical circuits in general, and particularly transistors, reached mesoscopic dimensions. A comprehensive introduction to transport in mesoscopic physics can be found in *Electronic Transport in Mesoscopic Systems* by S. Datta [3]. The following paragraph borrows heavily from its introductory remarks.

Where to use classical physics and where to use quantum mechanics is not evident. For conductors there are three characteristic lengths that can be used to determine whether the conductor behaves ohmic or not. These are the de-Brogle wavelength, the mean free path, and the phase relaxation length. If a conductor has dimensions significantly larger than these three lengths then

it can be considered macroscopic. The phase relaxation length is the average distance an electron can travel before it changes kinetic energy due to inelastic scattering processes. The mean free path is the distance an electron can travel in the material, before its initial momentum is destroyed due to scattering. Both the mean free path and phase relaxation length are dependent on the purity of the material and the temperature. A higher temperature gives a shorter mean free path. An example of a situation where temperature plays an important role in determining the model most useful is when considering a Bose-Einstein condensate (BEC). BECs are often dilute gases where a milli Kelvin temperature causes a material to start behaving non-classical. This exemplifies that going to a extreme can cause classical physics to stop to predict experiments accurately, even if the size is unchanged.

1.1 Nanowires

A Nanowire (NW) is an example of a system that can not be treated with ohmic laws. As the name implies a NW is a wire, conductor with diameter much smaller than its length, where the diameter is in the 1-100 nanometer range, $1\text{ nm} = 10^{-9}\text{m}$. As the Fermi wavelength of electrons in a semiconductor is on the order of the diameter, the transverse eigenenergy states play a large role in determining the transport properties of the system.

There exist a variety of applications in technology for NWs including creating NW field-effect transistors [4] [5] and sensors [6]. A more complete picture of the applications of NWs can be found in the review article [7]. There applications such as photonic, thermoelectric, photovoltaic, photoelectrochemical, battery, mechanical, and biological are discussed. In the quest for smaller and faster computers, much effort is focused on the applications in transistors. Standard consumer computers need to function at room temperatures, thus focus lies in effects seen at room temperature [8],[9].

At Lund University there are groups that experimentally create semiconductor NWs, for example [10]. A method to test properties of NWs is to attach metallic contacts to the ends of the wire and apply a voltage and measure the current.To get more information an electric field is applied, called gate voltage, raising the Fermi energy in the NW. It is results from conductance vs gate voltage measurements that this bachelor thesis aims to predict theoretically. Some success to model NWs within the theoretical model presented herein has been achieved [2] as a part of the same ongoing effort at Lund University to theoretically reproduce characteristics of experimental

mesurments of semiconductor NW systems.

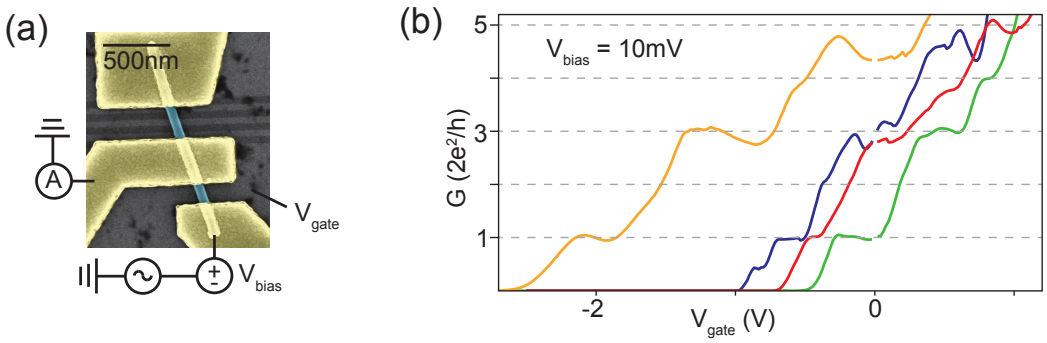

Figure 1 – Figure on the left is a typical experimental setup for measuring the conductance of a NW. The NW is placed on a isolating surface with metallic contacts placed around it on both ends. The gate voltage of the metal underneath a isolating substrate is changed to control the Fermi energy of the nanowire. (a) scanning electron microscope (SEM) picture of typical system. (b) the result of gate voltage vs conductance measurement. Figure from [11]

Quantized conductance has been achieved in 2 dimensional electron gases [12] and quantum point contacts [13]. However, it has been hard to produce experimental evidence for quantized conductance, that is the hallmark of ballistic transport, in semiconductor NWs. For an overview of why ballistic transport is expected and how quantized conductance arises see sections 2.1 and 2.3. Quantized conductance in InSb NWs has just recently been observed March 2016 [11]. Results from that paper is shown in figure 1. The search for quantized conductance in semiconductors further motivates theoretical study of the dependence of contact geometries on conductance, as it might be part of why it is elusive in experiments.

2 Method

To investigate the effects of contact geometries in NW experiments a method based on effective mass approximation (EMA) followed a by finite difference method (FDM) approximation and finally Landauer-Büttiker formalism has been used to calculate conductance. This section aims to provide a general idea of the method used and motivation for the choices made with regards to the method. Writing down the complete, exact Hamiltonian might be possible

but solving its eigenvalue equation analytically is most likely impossible. Even numerical solutions to that equation is generally impossible for multi particle systems of this size.

2.1 Effective Mass Approximation

Even though the spatial wavefunction of the crystal is not known, information about it can be gained through symmetry considerations. Assuming an infinite crystal, a particle subjected to a symmetry translation of the crystal will see the exact same surrounding as before, therefore it must be equally probable to find the electron at the two points. This implies that the square modulus of the wavefunction must be the same. Thus the wavefunction is a Bloch function. That is a periodic function multiplied with a phase factor in the form of a plain-wave function.

This symmetry property is then used, together with some approximations, to simplify equation to a form that give rise to the interpretation of the quasi-particle effective mass electron. As the name implies the effective mass electron has the same properties of the free electron but it has a different mass. The assumption made are that the electrons have energies close to the conduction band bottom. A band in a crystal is a finite interval of energies that an electron can have in the solid separated from similar bands by forbidden energy regions.

A way to visualize the EMA is to consider that the energy of an electron in the crystal depends on its wave vector. The energy as a function of the wave vector is a continuous twice differentiable function. A continuous twice differentiable function has derivative equal to zero at the minimum; thus the bottom of the band has a parabolic structure to third order. The relation between energy and wave vector for a free particle is $E_k = \frac{\hbar^2 k^2}{2m}$. If the energy is close to the band bottom, electrons can bee seen as free but with a changed mass.

This approach is called the effective mass approximation (EMA). The free particle behavior makes both analytical and numerical calculations significantly easier. The derivation of the EMA model is outside the scope of this thesis and can be found in [14].

The Hamiltonian of the system can now be written as the Hamiltonian of an electron confined inside the geometry of the system. Electron-electron interactions are neglected. This gives the Hamiltonian in equation 1. $V(r)$ describes the infinite potential walls that form the desired geometry. $\bigtriangledown^2$

is the Laplacian. m^* is the quasi-particle electron effective mass. r is the position operator.

$$H = \frac{-\hbar^2}{2m^*} \bigtriangledown^2 + V(r) \tag{1}$$

Unfortunately, NWs are different from an infinite crystal. Indeed what makes NWs interesting is that they are finite. So will a model based on infinite crystal structure give any relevant results? Theoretical studies have shown that when adjusting the effective mass for the smaller system, EMA can still produce results in agreement with a atomistic tight binding models (TBs) for nanowire systems [9]. Further, the comparison to TB models suggests a restriction that EMA only work for wires with diameter larger than 3-6 nanometers [9]. However, these diameters are for room temperature voltage vs current measurements so the applicability on low temperature conductance vs Fermi energy simulations can not be guaranteed. Still it provides a idea of at what diameters the EMA model describe relevant physical properties.

A TB model is used to motivate the choice of EMA. Therefore, there is a need to briefly describe the model and why it is not used instead of the EMA. The model is described in [9] as:

> Nearest-neighbor tight binding (TB) model ($sp^3d^5s^*$) [15] for electronic structure calculation, coupled to a 2D Poisson solver electrostatics.

The TB approach used in [15] is described in the introduction of that article as that the valence electron state is expanded in term of the local orbitals of the atoms. Later in the introduction however [15] explains this is not a complete basis and the parameters of the TB approach is determined semi-empirically from measurements on the bulk material in question. At the same time, the TB scheme is not as dependent on the infinite crystal scheme and is therefore a useful tool in assessing the validity of EMA at small diameters.

So why not use TB instead of EMA? The ultimate choice of EMA over TB comes down to three factors. Firstly, the most important reason is that a TB approach requires significantly more complex theory and hard work to be applied compared with EMA. Therefore, an endeavor to big to

be accomplished within the highly limited time frame of a 15hp (10 week) project.

Secondly, the effective mass approximation does not need to consider the atomic granularity of the nanowire more than by changing the effective mass. This of course a gross simplification and is not always applicable. Still an EMA code describes properties that many nano sized semiconductor system might exhibit. The TB code is highly material dependent and need to be rewritten for every crystal structure. The goal of this work is to investigate contact geometry effects. Therefore, it is reasonable to neglected effects of specific crystal structures and confine the domain of validity to the bottom of the band, in exchange for more generic results.

Thirdly, TB models are computationally much more expensive. [15] addresses this by developing the numerics to fit a specific type of computer cluster. The cost of computations have decreased considerably since the publication in 2002 (2016). However, the computational cost and time to implement such a solution is still considerable. When considering the computational cost in TB, the physical size of the system in itself becomes a problem fast. Searching the largest NW diameter claimed to have been simulated with a TB approach the largest diameter found in literature 40 nm [16]. Compare this with the diameter of 70-80 nm reported in [11] shown in figure 1 (a). With the added geometry of the contacts and simulation of systems as in 1 seem impossible at the moment.

When using a EMA model with a numerical solution to the differential equation the maximum size of the system that can be calculated is dependent on the desired maximum energy. This is due to the fact that the smallest "feature" of the wave function that need to be resolved is dependent on the energy.

Fortunately, when studying ballistic transport in nanowires, experiments only measure the conductance for a couple of conductance steps. The wave-functions of these states do not need more discretization points as the size increases for the same accuracy. For example the ground state of infinite potential well box is equally well represented with 10 points at any size of the box. This will also later be seen in the fact that the energy scale of simulations is dependent on the physical distance between discretization points. So if the numerics converge for one size of the system then it converges for all scaled up systems but for lower energies.

Further, the EMA becomes better when the energy is closer the band bottom. Thus this model even becomes more reliable for large wires when

only the first couple of conductance steps are investigated.

2.2 Finite Difference Method

For a simple geometry described by the potential $V(r)$, the EMA Hamiltonian in equation 1 in section 2.1can be treated analytically. However, using a finite difference method (FDM) discretization with the Kwant package makes handling of a multitude of geometries, in 2 and, 3 dimensions considerably more manageable. The 1D Hamiltonian will now be constructed as an example of how the FDM solution can be turned into a linear algebra problem. From there, necessary results for the implementation of a general multidimensional system in Kwant will be deduced.

$$\begin{aligned}
&\begin{cases} \Psi(x+a) = \Psi(x) + a\Psi'(x) + \frac{a^2}{2}\Psi''(x) + \mathcal{O}(a^3) \\ \Psi(x-a) = \Psi(x) - a\Psi'(x) + \frac{a^2}{2}\Psi''(x) + \mathcal{O}(a^3) \end{cases} \\
&\Leftrightarrow \Psi(x-a) + \Psi(x+a) = 2\Psi(x) + a^2\Psi''(x) + \mathcal{O}(a^3) \\
&\Leftrightarrow \Psi''(x) = \frac{1}{a^2}(\Psi(x-a) + \Psi(x+a) - 2\Psi(x)) + \mathcal{O}(a) \qquad (2)
\end{aligned}$$

From Taylor expansions, the expression for the second derivative in equation 2 is derived. A spatial wavefunction is only required to be twice differentiable but for the Taylor series to be valid the function must be infinitely differentiable. One way to deal with this problem is to conclude that we are indeed looking for a infinitely differentiable solution and that this solution is close to the EMA analytical solution. Further, it can be argued that as the Taylor series is truncated after the second derivative term, information of higher order derivatives are in some sense already lost.

The final expression in equation 2 is only dependent on three function values around the point of derivation with an error on the order of the step length a. Thus, as a tends to zero the error also tends to zero. Consequently, any desired accuracy can be achieved by choosing a small enough step length a. Note that the binary representation of numbers in a computer result in a non-zero inaccuracy. However, this inaccuracy is several orders of magnitude smaller than any inaccuracy of simulations presented in this thesis.

Let $\Psi_i = \Psi(ia), i \in \mathbb{Z}$ and let $\Psi = (\Psi_1, \ldots, \Psi_m)$ be the discretization of the continuous wave function on the interval $x \in [0, im]$. If we choose $V(x)$ as zero on the interval $[0, im]$ and infinite otherwise. Then the FDM

Hamiltonian can be expressed as the $m \times m$ matrix shown in equation 3. Note that $\Psi_{-1} = \Psi_{m+1} = 0$ as $V(-a) = V(ma + a) = \infty$.

$$H = t \begin{bmatrix} 2 & -1 & 0 & 0 & \dots & 0 \\ -1 & 2 & -1 & 0 & & \vdots \\ 0 & -1 & 2 & \ddots & 0 & 0 \\ 0 & 0 & \ddots & \ddots & 1 & 0 \\ \vdots & & 0 & -1 & 2 & -1 \\ 0 & \dots & 0 & 0 & -1 & 2 \end{bmatrix} \tag{3}$$

$$t = \frac{\hbar^2}{2m_e^* a^2} \tag{4}$$

Creating the matrix in 1D is relatively simple but the task becomes difficult in higher dimensions and for complex geometries. Note that the Laplacian is the sum of several second order derivatives on the form of equation 2. The term $\Psi(r)$ is called the onsite term. The terms $\Psi(r + \delta)$ where δ is a unit vector times a are called hoppings. The onsite term will be multiplied with $2dt$. With d being the dimension. The hopping elements between sites will all be multiplied with $-t$ independent of dimension. For convenience we choose $t = 1$.

The length unit used in presenting the size of systems in the results section, and in figure 3 is arbitrary and will only be presented as numbers without unit. The result of different length unit choices results in a changed energy scale. The energy unit is t with a equal to the length unit. For example, choose the length unit to be nanometers in an InSb nanowire with effective mass ratio $\frac{m^*}{m_e} = 0.017 \pm 0.007$ [17], where m_e is the electron mass. This results in $1t = 2.24$ electron volts. When using different discretizations all results are normalized to fit this length unit by changing the t used in simulations.

To guide the initial choice of the discretization length a for a specific system it is helpful to consider what it is that the discretization aims to resolve. The eigenvectors of the discretized Hamiltonian are the spatial representations of the eigenenergy states. And for the results from manipulation of this Hamiltonian matrix it is reasonable to assume that the structure of the eigenvectors must be resolved. Thus the discretization need to resolve the spatial wavefunction of the system.

2.3 Kwant

To calculate the transmission probability for complex geometries, and to facilitate efficient calculations, the Kwant package is used. Kwant is described on the Kwant home page (April 2016) as:

> Kwant is a free (open source) Python package for numerical calculations on tight-binding models with a strong focus on quantum transport. It is designed to be flexible and easy to use.

Kwant can handle all TB models. However, Kwant also makes it possible to implement a FDM-discretized Hamiltonian in Kwant as mentioned in the paper introducing Kwant [1], and in section *2.2. First steps: setting up a simple system and computing conductance* in the Kwant documentation (April 2016).

Implementing a 3D FDM in Kwant using the same approach as described here was done in a bachelor thesis at Lund university as a part of the same ongoing effort to describe experimental results [2]. As shown in figure 2 from [2], a FDM scheme implemented in Kwant indeed came close to an analytical solution in a situation where such a solution could be produced. [2] analyses the impact of the geometry of the nanowire, effects of a Gaussian disorder model (GDM), and the effect of a uniform magnetic field, within the EMA model. This thesis investigates lead geometry effects and the wire geometry is chosen to be hexagonal in the 3D geometry. The choice between hexagonal and circular cross section of the NW do not significantly change the properties [2].

To be able to model contacts, Kwant can handle semi-infinite systems with translation symmetry. A NW can bee seen as a finite scattering region, with semi-infinite leads attached to it representing the contacts in the experiments. Kwant demands that the leads must have translational symmetry. The Kwant package has methods for calculating the scattering matrix and in turn the transmission coefficients on the form $\hat{T}(E)$ from equation 8 presented in section 2.3.

The scattering matrix is a matrix that act as a linear map between incoming states and outgoing states in the leads. The number of operations needed to define the system scales linearly with the system size but the number of operations needed for calculating the scattering matrix scales with the number of points in the system given by equation 5 [1]. n is the number of points and d the dimensionality of the system.

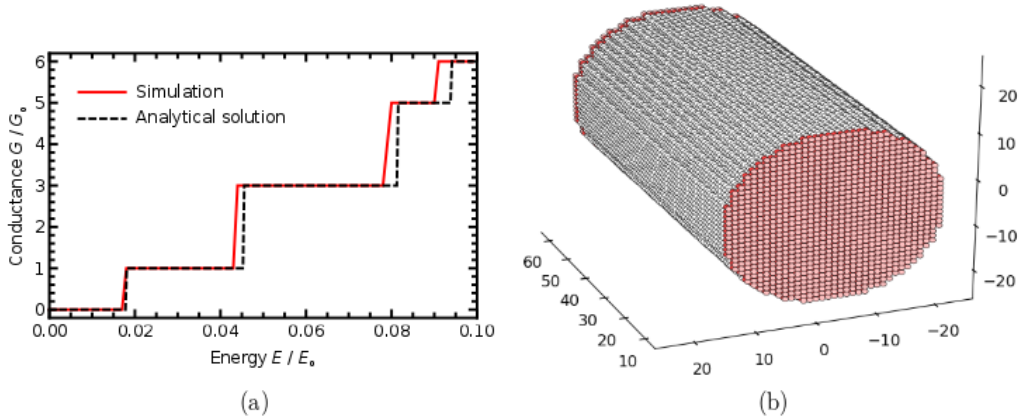

Figure 2 – (a) Simulation results and comparison to analytical solution for the conductance of the circular nanowire described in Section 5.1 of [2]. (b) A visualization of the model used to numerically simulate the nanowire. Red regions represent semi-infinite leads. Figure is from [2]

$$\text{Number of operations} = \mathcal{O}(n^{3-2/d}) \tag{5}$$

3D models in Kwant are thus more computationally intense, both due to the increased number of points needed to discretize a volume compared to a plane, but also the time needed to compute the scattering matrix as the number of points in the system increase is dependent on dimension.

Therefore, 2D models are less computationally intense and facilitate a more simplistic construction and analysis of data than 3D models. However, the process of reducing a 3D structure to a 2D structure inevitably destroys some of the information about the system. Simulations are made on both a 2D projection and a full 3D geometry to make use of the advantages of both models.

The poor scaling of the scattering matrix calculations implies that as the size of the system goes to infinity, the fraction of time spent in the calculation of scattering matrices goes to 1. Thus, for large systems the efficency of the implementation of the definition of the system is not important. Further, costly matrix manipulations can be executed with the help of external optimized libraries written in a low level language for speed. Consequently, Kwant has similar performance as libraries written in pure C and FORTRAN, despite

being written in the high-level language Python. Simply because most of the time is not spent executing python code.

The way to model the contact geometries in systems like that in figure 1 is not evident. The aim of this modeling is to capture essential physical properties of the contact geometry. An obstacle in this pursuit is that the contacts are metallic and therefore have a much shorter Fermi-wavelength. A geometry property of the contact geometries of these systems is that the contacts are attached around a section of the nanowire. In 3D this is modeled by attaching three leads to each end of the nanowire. One on top and one on each side. A visualization of that system can be found in figure 3 (b). The 2D projection is found in figure 3 (a).

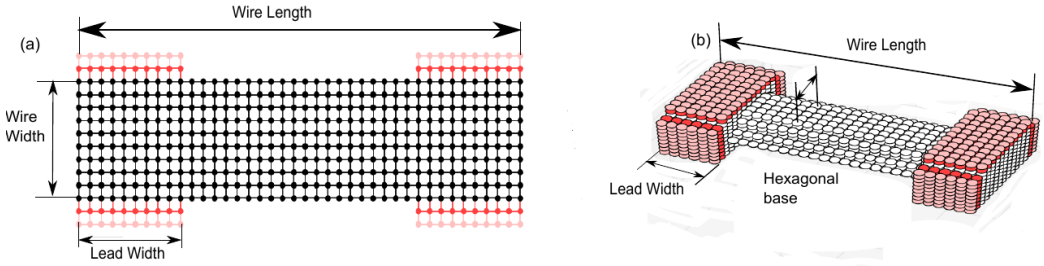

Figure 3 – Visualizations of 2D and 3D models in Kwant. Semi-infinite leads are plotted in red. (a) 2D system with four leads. Wire width 10, lead width 10, and wire lead width 10. (b) 3D system with 6 leads. Hexagonal base 5, lead length 6, and wire length 30.

The lower computational cost when dealing with 2 dimensional models gives opportunity to push the FDM convergence closer to the EMA solution. However, a 3 dimensional model can incorporate more geometric characteristics of the wire. One such characteristic that 3D can incorporate is the effect of having leads on all but the side facing the underlying isolating substrate. Kwant has implemented methods to calculate the transmission $\hat{T}(E)$ at a specific energy E. This transmission function is the result presented in the result section. The next section will deal with the physical meaning of this transmission function.

2.4 Landauer-Büttiker formalism

It may seem trivial that the probability of transmission is linked to the conductance, and indeed this is the case. But the actual theory is not trivial

and can be understood through the Landauer approach. A more complete derivation of the Landauer-Büttiker formalism can be found in section 2 of [3]. The derivation is outside the scope of this thesis and the results of that derivation will be presented herein with only meager motivation.

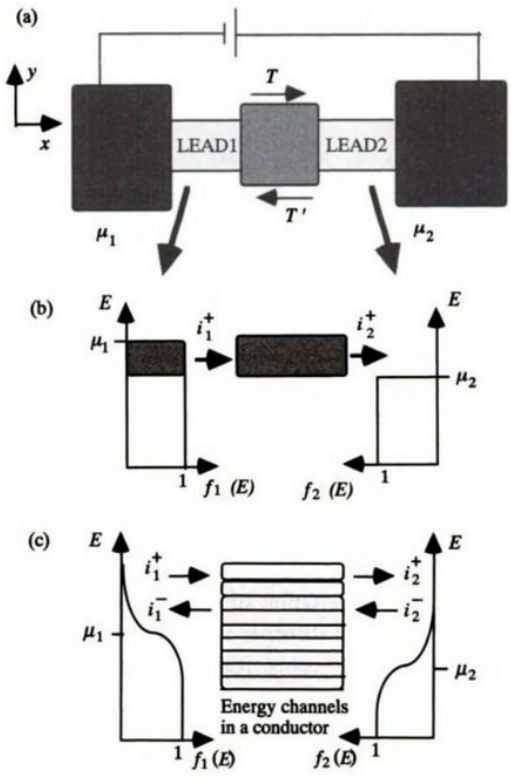

Figure 4 – (a) A conductor is connected to two large contacts through leads. (b) Energy distributions of the incident electrons in the two leads at zero temperature. (c) Energy distributions at non-zero temperatures. Figure and caption from [3]

Consider a ballistic mesoscopic wire between two large conductors with chemical potentials μ_1, μ_2 and temperature 0 T. Ballistic behavior implies that electrons can flow without scattering in the wire. The wire will have transverse states corresponding to "particle in a box" energies each creating a mode. This results from that the wave function can be split into a transversal and longitudinal part. Assuming reflectionless contact surfaces it can be shown that each mode carries the same amount of current independent of

each other. Giving the conductance in equation 6.

$$G_c = \frac{2e^2}{h} M \tag{6}$$

This phenomenon is called quantized conductance and efforts observing it experimentally are discussed in section 1.1. M is the number of accessible modes and G_c the conductance through the wire. Note that as the wire is ballistic the voltage drop inside the wire is zero and all the resistance is in the contact-wire interface. Note that as the width of the wire increases the number of open modes in the wire increases as well and the conductance increases. This resistance is thus zero for macroscopic conductors where $M \to \infty$. However, other sources of resistance exist and instead become dominant for large M.

If a scattering region is introduced as in figure 4 (a) the conductance also becomes dependent on the transmission probability through the scattering region. Assuming that the transmission T is constant on the interval $[\mu_1, \mu_2]$, which is only true for infinitesimal intervals. Further, the transmission coefficient is assumed to be symmetric with respect to direction. That is $T = T'$ in figure 4. This situation is depicted figure 4 (b). The conductance is with these assumptions given by the Landauer formula in equation 7.

$$G = \frac{2e^2}{h} MT \tag{7}$$

At a finite temperature and bias as depicted in figure 4 (c) more is needed. Further, also the energy dependency of the transmission function need to be addressed. By expressing the incoming influx and the outflux of the leads in terms of number of open modes and transmission probability at that energy the net current can be calculated to be $i(E) = \frac{2e}{h} M(E)T(E)[f_2(E) - f_1(E)]$ at energy E. f_1, f_2 are Fermi-Dirac distribution functions.

If the voltage drop introduced by a finite bias occurs inside the scattering region the transmission coefficients may change. There is reason to suspect that this finite bias effect will be negligible for small enough biases. However, when dealing with large biases these effects may very well cause non-negligible changes in the transmission function. Modeling this voltage drop is thus needed for high bias.

To get the total current, the net current is integrated over all energies, $I = \int_0^\infty i(E)dE$. Extending this reasoning to multi-lead systems as in figure

3, the total net current is instead the sum of all net currents between the right leads in the system and left leads as seen in equation 8. $\hat{T}(E) = M(E)T(E)$ is the result of numerical simulations.

$$I_p = \int i_p(E)dE \ , \ i_p = \frac{2e}{h} \sum_q \hat{T}_{pq}(E)[f_p(E) - f_q(E)]dE \tag{8}$$

With this final step, from transmission function to current ,a method to numerically calculate the conductance $G = \frac{I}{\mu_1 - \mu_2}$ is introduced. This model can handle non-zero temperature, low finite bias, and complicated geometries.

3 Results

3.1 2D systems

3.1.1 Numerical stability

As the ratio of discretization length over Fermi wavelength approaches zero the numerical solution converge to the solution of the EMA model. To test how close to the EMA-analytical solution the numerical solution is, the discretization step is reduced by a factor 2 multiple times. Figure 5 show the result of such simulations. The solution is stable and appear to be converging even though for energies larger than $0.4t$, the solution is less stable. The convergence suggests that the numerical solution is close to the analytical EMA-solution limit for energies lower than $0.4t$. It is worth noting that the peaks in conductance move to higher energies as the discretization is increased. This is a recurring property of the numerical solution also seen in the figure 2 and 9. This simulation suggests that the numerical solution is close the EMA-limit.

3.1.2 Lead width effects

The results from simulations with different lead widths, as defined in figure 3, are presented in figure 6. From "particle in a box" solutions, the analytical leads modes can be calculated. In figure 6 it is clear that the onset of a new mode in the lead and zero transmission are correlated suggesting a dependence. However, the contacts in experiments are metallic with a different effective mass compared to the semiconductor material of the nanowire. This implies

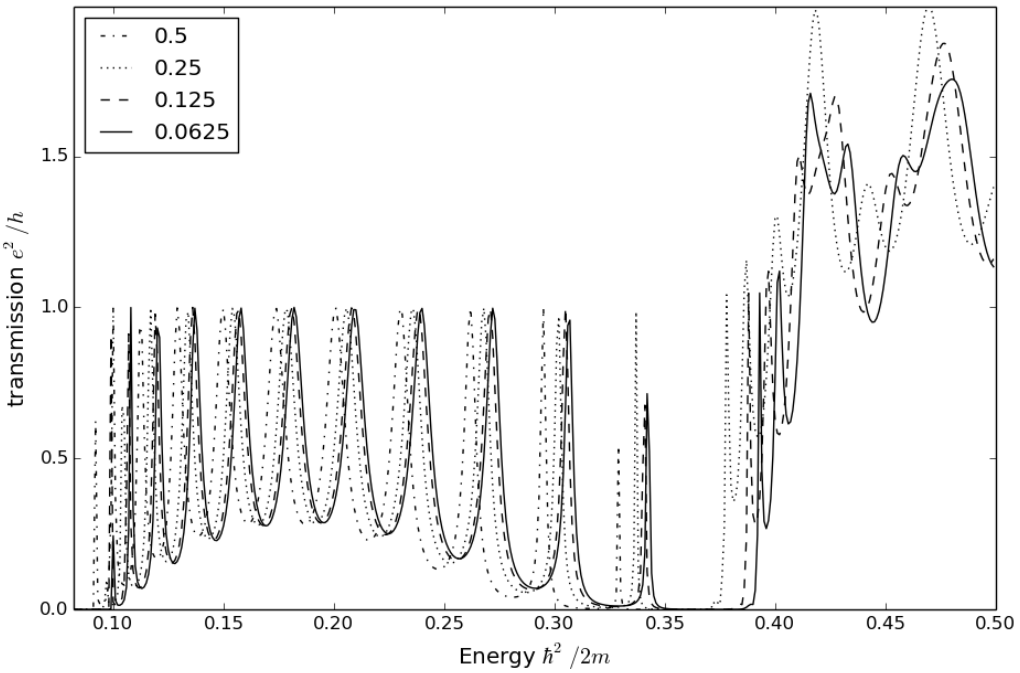

Figure 5 – Discretizaton test of systems with 4 leads in 2D systems as in 3 (b) with discretization step length 0.5, 0.25, 0.125, and 0.0625. Wire base 10, lead width 10, and wire length 80. In arbitrary length units.

that the energies of the transversal states in the leads are *not* corresponding to that of a metallic contact.

The straight forward way to solve this problem is by introducing a position dependent effective mass. This would in some sens correct the lead mode energies. Further, a position dependent effective mass has the potential to better model the metal semiconductor interface.

Further, if the wire had no leads connected, the analytical values of its eigenenergies are the "particle in a 2D box" eigenenergies. The system indeed has leads, thus correlations in the order of numerical convergence to effect dependent on analytical "box" energies of the wire can not be expected.

3.1.3 Lead interface potential barriers

The wire is not a closed finite box, but it can be made more like such a system by adding potential barriers at the lead-scattering region interface.

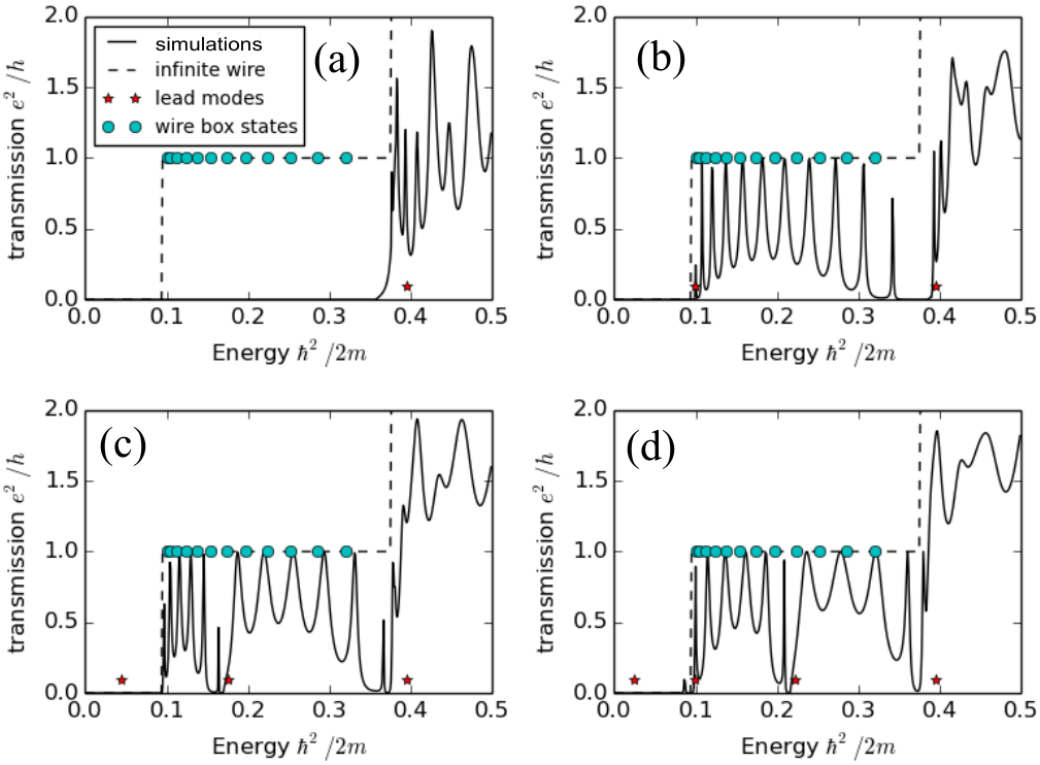

Figure 6 – Energy vs conductance for systems of same type as in figure 3 (a) with different lead widths (W). Wire width 10 and total length 80. Discretization length is 0.25. Stars are placed at the analytical values retrieved when calculating the transversal energy states in the leads. The circles are placed at the analytical eigenenergies of the wire without leads. Plots have the following lead widths: (a) W = 5, (b) W = 10, (c) W = 15, (d) W = 20

The result of such simulations are found in figure 7. An increased potential barrier causes resonance peaks to become more narrow. This effect is similar to that of resonances in a 1D double barrier system. The similarity suggests that states similar to the eigenenergy states in the closed wire act as resonances in the open wire.

The movement of resonances can initially cause confusion as the first zero barrier resonance is not present due to the fact that the energy of that resonance is situated below the onset of the first mode in the leads. It is thus necessary to consider the missing first resonance to identify the corresponding closed wire state. A barrier of height 10 moves the state considerably up in

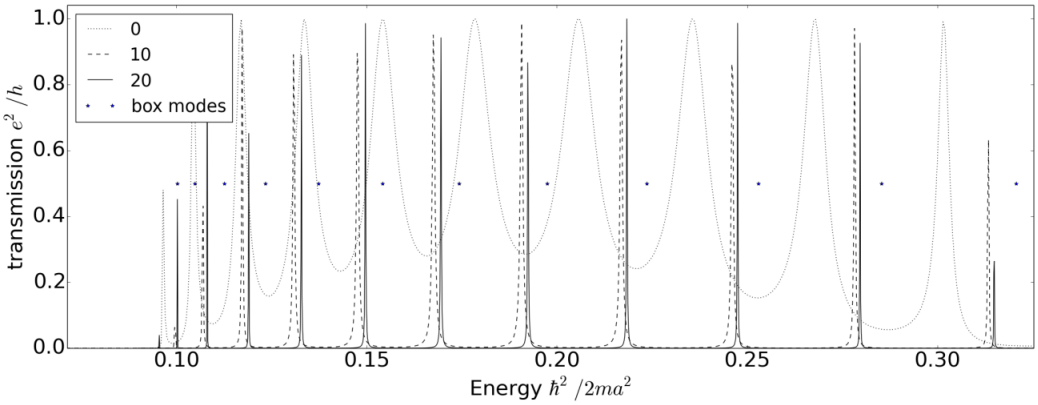

Figure 7 – Effect of potential barriers at the lead-scattering region interface on transmission as a function of energy. 2D system with wire length 80, wire width 10, and lead width 10. A potential barrier of arbitrary units with height 0, 10, 20 is applied in the border between the lead and the scattering region. Note that the barrier is applied to only one site in the simulation and thus the number that describe the height is highly dependent on the discretization of the system.

energy. This can also be expected when considering a particle in a 1D box with finite potential walls. Higher potential walls increase the bound state energies as the particle is effectively confined in a smaller space. This can also be said about the wavefunction inside the wire.

For the barrier of height 20 the position is *not* moved significantly closer to the analytical result. This suggests a convergence to a value different from the analytically predicted resonant energy. This is attributed to the finite discretization that results in lower eigenenergy values as described earlier in this section. To further validate this conclusion a simulation with reduced step length could be made. Due to the large number of points needed to resolve the resonance peaks this becomes a demanding simulation. As this behavior of the FDM solution has been validated in figure 5 such validating simulations have not be conducted. The results of the simulations made in this thesis suggest that the conductance resonance peaks are indeed an effect of the finite length of the wire.

Finally, the height of the resonance peaks seem to decrease with increased barrier height. This phenomena is likely a result of the finite number of points in which the transmission function is sampled. In figure 7 the number of

sampled points is on the order of 2700, with increased point density near the onset of the first lead mode. However, some peaks are still only sampled with 2-3 points. Calculating the transmission in this number of points is only possible due to the less computationally intense 2D model.

3.1.4 Reappearance of conductance steps

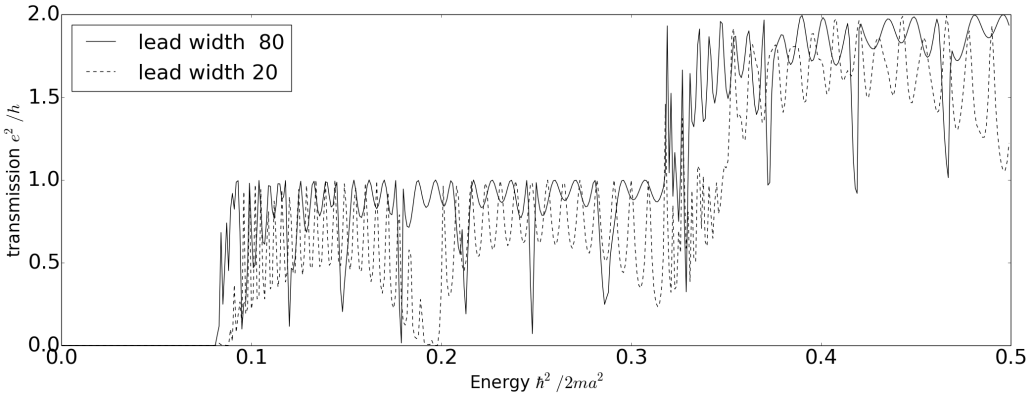

Figure 8 – 2D system with increased lead width from 20 to 80. Wire length 320, and wire width 10

When comparing figure 8 with figure 6 it is clear that a large wire length increases the number of resonances as expected. Further, as both wire length and lead width is increased the transmission function comes closer and closer to the transmission step function. The effect of the lead modes reduces to inducing highly localized zero points. These points will not influence the resulting conductance when introducing a finite bias and temperature that "smears" out the transmission function [2].

3.2 3D systems

In figure 9 the system with length 30 and hexagon base of 10, with discretization 2, 1 and, 0.5 points per length unit has 2 000, 8 000, and 31 000 points respectively. A 3D system in Kwant scales as $n^{1.34}$ with the number of points, from equation 5. Also, the number of points increase with the cube of the discretization, thus the computational time increases like $\mathcal{O}(n^{4.334})$ with reduced discretization. For example, a factor 2 reduction in discretization length increases the computational cost with a factor 20. However, the result of the discretization test in figure 9 presents a satisfactory rate of convergence.

The 2D case, as expected outperforms the 3D case in the sens of numerical convergence to the EMA analytical results. This is expected as the computational cost increases like $\mathcal{O}(n^3)$ in 2D systems compared to $\mathcal{O}(n^{4.334})$ in 3D. This makes it possible to have a better ratio between discretization length and wave length in 2D systems.

Nonetheless, for the first two conductance steps in figure 9 the numerical solution is stable. Thus, there is reason to suspect that the numerical model is in at least qualitative agreement with the EMA model.

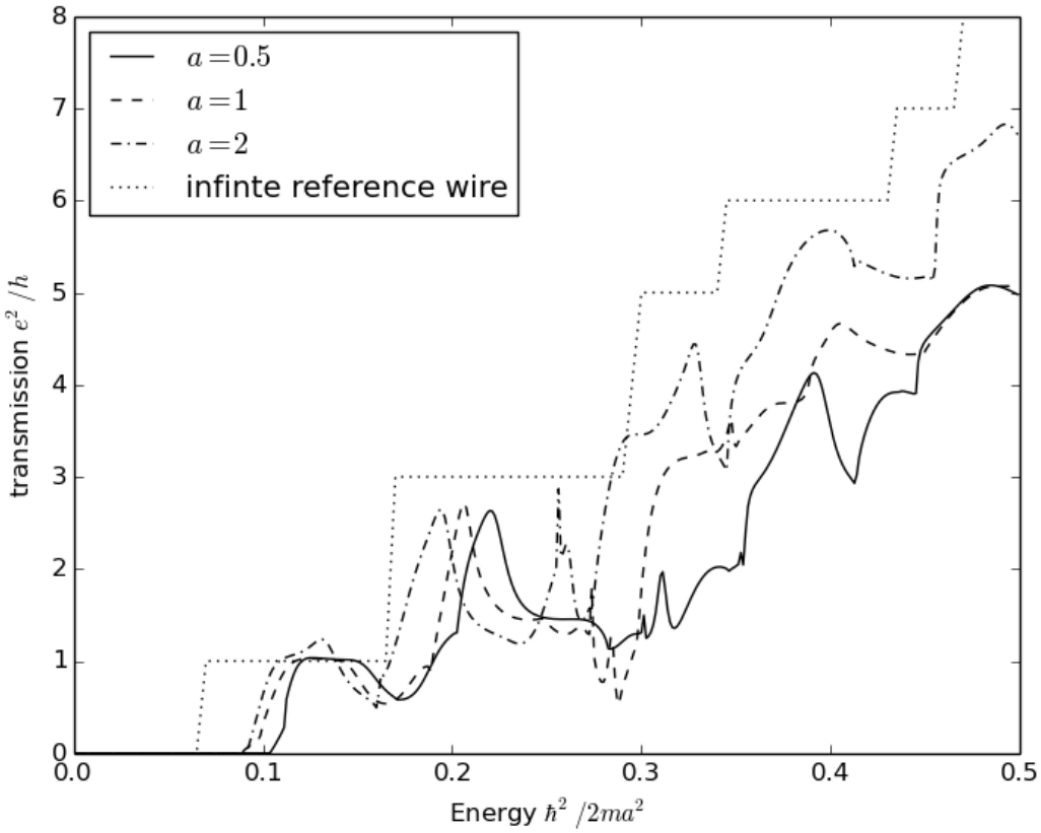

Figure 9 – Discretizaton test of 3D system as in figure 3 (c). System length 30, base of hexagon 10 and contact length along wire 10. Discretization step 2, 1 and, 0.5.

The experimental results presented in section 1.1, figure 1 have some similar qualitative behavior as that of the first two steps in figure 9. The conductance seem to drop at the end of the conductance step both in these EMA simulations

and in the experimental data. There is currently no convincing qualitative analytical argument within the EMA model for its appearance.

The results presented herein do not include the effects of finite temperature and bias. From equation 8 and figure 4 in section 2.3 the effect of finite temperature is to "smear" the steps by a symmetrically weighted integral. The effects of temperature and bias on transmission have been investigated in [2]. In the case of an attempt to do a quantitative match to experimental values temperature and bias would be included as in equation 8.

The onset of the first and second conductance step in figure 9 is higher in energy than the infinite wire. The first and second analytical mode energies of the leads have energy 0.1 and 0.2 in the energy unit $t = \frac{\hbar^2}{2m^* a^2}$ from equation 4. As the onset of the first mode in the scattering region occurs before the first mode in the lead is avaliable there is no conduction up to this point. As discussed earlier the energies of these lead modes have no physical significance due to that the model in some sens treating the metal like the semiconductor material of the nanowire.

4 Outlook

In the leads of figure 3 (a) and (b), the energy of transverse modes in the leads will be dependent on the width of the leads and the effective mass. As the effective mass in those leads does not correspond to the effective mass in the metallic leads, the energy of the transversal modes is not correct.

To address this issue, the effective mass could be made position dependent in the system. This could be done by having a different value of the t variable in different parts of the system Another way could be to abandon the EMA model for TB models. However, as discussed extensively in the EMA section of this thesis this would dramatically restrict the maximum size of the system.

A larger effective mass leads to a smaller wavelength of the effective mass electrons. A larger number of discretization points are needed to describe a wave function with smaller wavelength. Using this smaller discretization length in the entire system would be computationally costly. Therefore, different discretizations in leads and scattering regions is needed.

For simple systems there exist analytical solutions to the position dependent effective mass (PDEM) problem. The PDEM problem of an infinite 2D wire with an abrupt change in effective mass was studied with boundary condition derived in [18].

Unfortunately, for a naive implementation of PDEM in the FDM scheme in Kwant the analytical case did not agree with the corresponding numerical simulation. It is likely that a solution to implement a FDM scheme in 2 and 3 dimensions can be found as a solution in 1D has been found [19]. Further, FDM is an often used method and PDEM is a common situation in semiconductor simulations.

Further, after implementing the PDEM a comparison with experimental data is the next step. As the dimensions of devises, as well as energies have wide margins, constructing an algorithm to minimize the discrepancy between simulations and experimental results by changing model parameters such as dimensions and effective masses would save much time. This would put the model, to its ultimate test. The test of agreement with experimental observations.

References

[1] Christoph W Groth, Michael Wimmer, Anton R Akhmerov, and Xavier Waintal. Kwant: a software package for quantum transport. *New J Phys*, 16(6):063065, 2014.

[2] Oscar Erlandsson. Numerical simulations of quantum transport in semiconductor nanowires, 2016. Student Paper.

[3] S. Datta. *Electronic Transport in Mesoscopic Systems*. Cambridge Studies in Semiconductor Physi. Cambridge University Press, 1997.

[4] Yi Cui, Zhaohui Zhong, Deli Wang, Wayne U. Wang, , and Charles M. Lieber*, . High performance silicon nanowire field effect transistors. *Nano Lett*, 3(2):149–152, 2003.

[5] Jean-Pierre Colinge, Chi-Woo Lee, Aryan Afzalian, Nima Dehdashti Akhavan, Ran Yan, Isabelle Ferain, Pedram Razavi, Brendan O'Neill, Alan Blake, Mary White, Anne-Marie Kelleher, Brendan McCarthy, and Richard Murphy. Nanowire transistors without junctions. *Nat Nano*, 5(3):225–229, 2010.

[6] Yi Cui, Qingqiao Wei, Hongkun Park, and Charles M. Lieber. Nanowire nanosensors for highly sensitive and selective detection of biological and chemical species. *Science*, 293(5533):1289–1292, 2001.

[7] Neil P. Dasgupta, Jianwei Sun, Chong Liu, Sarah Brittman, Sean C. Andrews, Jongwoo Lim, Hanwei Gao, Ruoxue Yan, and Peidong Yang. 25th anniversary article: Semiconductor nanowires synthesis, characterization, and applications. *Adv Mater*, 26(14):2137–2184, 2014.

[8] Nguyen Hong Quang, Ngo Trung Truc, and Yann-Michel Niquet. Tight-binding versus effective mass approximation calculation of electronic structures of semiconductor nanocrystals and nanowires. *Comput Mater Sci*, 44(1):21 – 25, 2008. International Conference on Materials for Advanced Technologies 2007 (ICMAT 2007) Selected papers of Symposium O: Frontiers in Computational Materials Science.

[9] Neophytos Neophytou, Paul Abhijeet, Mark S. Lundstrom, and Gerhard Klimeck. Simulations of nanowire transistors: atomistic vs. effective mass models. *J Comput Electron*, 7(3):363–366, 2008.

[10] Carina Fasth, Andreas Fuhrer, Mikael T. Bjrk, and Lars Samuelsonxs. Tunable double quantum dots in inas nanowires defined by local gate electrodes. *Nano Lett*, 5(7):1487–1490, 2005.

[11] Jakob Kammhuber, Maja C Cassidy, Hao Zhang, Önder Gül, Fei Pei, Michiel WA de Moor, Bas Nijholt, Kenji Watanabe, Takashi Taniguchi, Diana Car, et al. Conductance quantization at zero magnetic field in insb nanowires. *Nano Lett*, 2016.

[12] B. J. van Wees, H. van Houten, C. W. J. Beenakker, J. G. Williamson, L. P. Kouwenhoven, D. van der Marel, and C. T. Foxon. Quantized conductance of point contacts in a two-dimensional electron gas. *Phys Rev Lett*, 60:848–850, 1988.

[13] B. J. van Wees, L. P. Kouwenhoven, E. M. M. Willems, C. J. P. M. Harmans, J. E. Mooij, H. van Houten, C. W. J. Beenakker, J. G. Williamson, and C. T. Foxon. Quantum ballistic and adiabatic electron transport studied with quantum point contacts. *Phys Rev B*, 43:12431–12453, 1991.

[14] Yoshimasa Murayama. *Mesoscopic Systems: Fundamentals and Applications*, pages 187–190. Wiley-VCH Verlag GmbH, 2007.

[15] Gerhard Klimeck, Fabiano Oyafuso, Timothy B Boykin, R Chris Bowen, and Paul von Allmen. Development of a nanoelectronic 3-d (nemo 3-d)

simulator for multimillion atom simulations and its application to alloyed quantum dots. *Comput Model Eng Sci*, 2002.

[16] Y. M. Niquet, A. Lherbier, N. H. Quang, M. V. Fernández-Serra, X. Blase, and C. Delerue. Electronic structure of semiconductor nanowires. *Phys. Rev. B*, 73:165319, Apr 2006.

[17] R. J. Sladek. Effective masses of electrons in indium arsenide and indium antimonide. *Phys. Rev.*, 105:460–464, Jan 1957.

[18] Liès Dekar, Lyazid Chetouani, and Théophile F. Hammann. Wave function for smooth potential and mass step. *Phys. Rev. A*, 59:107–112, 1999.

[19] IH. Tan, G. L. Snider, L. D. Chang, and E. L. Hu. A selfconsistent solution of schrdingerpoisson equations using a nonuniform mesh. *J Appl Phys*, 68(8):4071–4076, 1990.